

# InAs/InP single quantum wire formation and emission at 1.5 $\mu\text{m}$

B. Alén,\* D. Fuster, Y. González, and L. González  
 IMM, Instituto de Microelectrónica de Madrid (CNM,  
 CSIC), Isaac Newton 8, 28760 Tres Cantos, Madrid, Spain.

J. Martínez-Pastor

ICMUV, Instituto de Ciencia de Materiales, Universidad de Valencia, P.O. Box 2085, 46071 Valencia, Spain.

(Dated: April 24, 2019)

Isolated InAs/InP self-assembled quantum wires have been grown using *in situ* accumulated stress measurements to adjust the optimal InAs thickness. Atomic force microscopy imaging shows highly asymmetric nanostructures with average length exceeding more than ten times their width. High resolution optical investigation of as-grown samples reveals strong photoluminescence from individual quantum wires at 1.5  $\mu\text{m}$ . Additional sharp features are related to monolayer fluctuations of the two dimensional InAs layer present during the early stages of the quantum wire self-assembling process.

PACS numbers: 81.07.Vb, 78.67.Lt, 73.21.Hb

Due to their smaller lattice and energy gap mismatch, InAs nanostructures grown on InP substrates are initially much better suited to exploit the long wavelength telecom windows than their GaAs counterparts. However, like the latter, to fulfill the requirements of solid-state based quantum information technologies, they have to be produced with low areal densities and high emission efficiencies. In this direction, emission from single self-assembled InAs/InP quantum dots (QDs) and dashes has been reported.<sup>1,2,3,4,5</sup> Under certain growth conditions and epitaxial methods, self-assembled quantum wires (QWRs) can also be obtained depositing InAs on InP.<sup>6,7,8,9,10</sup> Depending on the wire size and composition, emission tuning capability in the 1.2 - 1.9  $\mu\text{m}$  range has been demonstrated, and both, continuous wave and time-resolved optical characterization, have been performed on high density QWR arrays.<sup>11,12,13,14</sup> In such situation, long wavelength emission from single QWRs would be desirable. However, for the time being, single quantum wire optical spectroscopy has been restricted mainly to GaAs/AlGaAs nanostructures emitting on the visible range. The best examples are cleaved edge overgrown T-shaped QWRs,<sup>15,16</sup> V-grooved QWRs grown on nonplanar substrates,<sup>17,18</sup> and recently reported, vertical QWRs grown on inverted tetrahedral pyramids etched away on GaAs substrates.<sup>19</sup>

By using *in situ* accumulated stress measurements, the initial phases of the self-assembling process can be monitored during solid source molecular beam epitaxy (MBE) of InAs on InP(001).<sup>20</sup> We have exploited this fact to choose the optimal InAs deposited thickness and tailor the QWR areal density from zero to full coverage of the sample surface. A detailed study of the initial stages of QWR formation will be provided elsewhere. In the following, using a low areal density sample, we show experimental evidences of single InAs/InP QWR emission at  $\sim 1.55 \mu\text{m}$ .

The sample studied in this work consist of 1.5 ML of InAs (1 ML InAs = 3.03 Å) deposited on InP (001) at

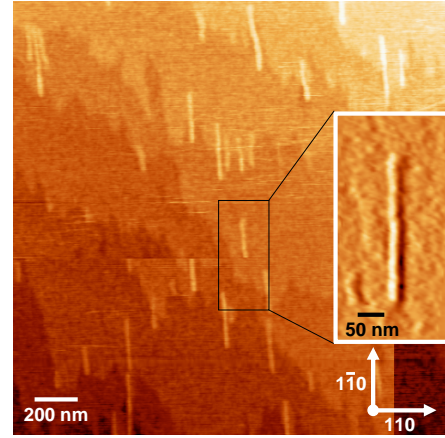


FIG. 1:  $2 \times 2 \mu\text{m}$  AFM image of the uncovered sample surface after deposition of 1.5 ML of InAs. Self-assembled quantum wires and one-ML-high InAs steps appear seldom distributed over the flat InAs surface. Inset: Zoom over a region containing a long QWR (first derivative image mode).

$r_g=0.5 \text{ ML/s}$ , substrate temperature  $T_S=480 \text{ }^\circ\text{C}$  and beam equivalent pressure  $BEP(As_4)=6.4 \times 10^{-6} \text{ mbar}$ . A 180 nm-thick buffer layer was deposited and before the In cell was opened again for InAs growth, the InP surface was exposed to As flux during 3 s. After QWRs formation, a 20-nm-thick cap layer was deposited at the same  $r_g$  to allow for optical investigation. In addition, an uncapped sample was grown under the same conditions for atomic force microscopy (AFM) investigation.

A conventional low magnification setup and non-resonant excitation at 514.5 nm have been used to study the ensemble averaged photoluminescence (PL) spectrum at 15 K. The collected light was detected synchronously by a Ge cooled photodetector attached to a 0.22 m focal length monochromator. The optical emission spectra at the single QWR level have been investigated using a confocal microscope working at 4.2 K (Attocube CFM-

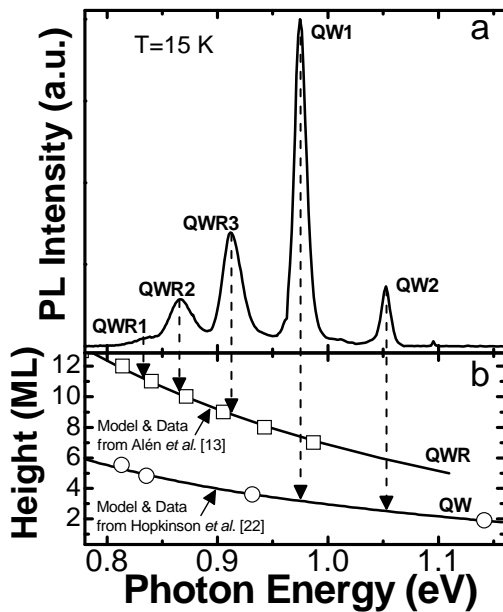


FIG. 2: a) Photoluminescence spectrum obtained at 15 K using an standard low magnification setup. b) PL energy vs. QW/QWR height dispersion curves have been extracted from previous studies. The energy position of the present emission bands are indicated by down-arrows in the corresponding curve.

I). Low level light detection has been achieved using a nitrogen cooled InGaAs focal plane array (Jobin-Yvon IGA-3000) attached to a 0.5 m focal length grating spectrograph. For this study, light excitation at 950 nm was delivered by a Ti-Sapphire tunable laser.

Figure 1 shows an AFM image of the uncovered sample surface. Elongated nanostructures appear randomly distributed with an average areal density of  $\sim 6 \mu\text{m}^{-2}$ . Statistics performed in more than 50 of such nanostructures reveal average widths and lengths of  $21 \pm 3$  nm and  $185 \pm 50$  nm, respectively. We note that, although the average aspect ratio is  $\frac{L_y}{L_x} \sim 8$ , QWRs with larger anisotropy ( $> 16$ ) can be easily found as shown in the inset of Figure 1. The low QWR areal density allows a direct analysis of the surface morphology underneath them. We observe a flat surface with one-monolayer-high steps due to the unintentional miscut angle of the InP(001) wafer ( $\sim 0.06^\circ$  off). In most cases, nucleation of the self-assembled nanostructures occurs preferentially in the step edges. However, a number of QWRs have been also found in flat areas far from any terrace border. The most remarkable observation is that, despite the orientation of the neighbor terrace step, QWRs growth occurs always along the  $[1\bar{1}0]$  direction. To this respect, any dependence among the QWR formation mechanism and the precise wafer miscut angle can be ruled out in our case.

It should be noted that with 1.5 ML of InAs deposited, plus an additional ML resulting from the As/P exchange

process,<sup>21</sup> the sparse QWR nucleation can not exhaust the initial InAs two-dimensional layer. In these conditions, a thin wetting layer must remain over the sample surface like usually observed for other self-assembled nanostructures. These low density QWR samples show optical features that can be related to an extended wetting layer of fluctuating thickness consistent with the amount of InAs deposited and the AFM characterization shown above. We must remark that the corresponding bands (QW1-2) dominate the PL spectrum for low InAs coverage and low QWR densities, but are effectively quenched when the QWR density is higher. They are hence strongly related to the incomplete self-assembling process occurring in this case.

The sample PL spectrum consists of five emission bands independently of the excitation power. A multimodal hypothesis can explain this behavior assuming that each band corresponds to QWRs or quantum wells (QWs) of a given constant height.<sup>11,13</sup> Figure 2(b) contains theoretical predictions and experimental data for both InAs/InP QWRs studied before by the authors,<sup>13</sup> and InAs/InP strained QWs grown and characterized by Hopkinson *et al.*<sup>22</sup> The solid lines represent the expected energy dispersion as calculated by the respective authors. We start associating the lowest energy band in the spectrum of Figure 2(a) to especially thick QWRs. They are rare in the ensemble distribution in view of the weak intensity of the corresponding PL peak (QWR1, 2 % of the total integrated intensity). Comparing with the QWR dispersion curve shown in Figure 2(b), we observe that its emission energy, marked with a downarrow, agrees well with 11-ML-thick quantum wires. Peaks labelled as QWR2 (13 %) and QWR3 (26 %) also agree with data collected in high density samples for 10 ML and 9 ML thick nanostructures, respectively. The series is suddenly cut off since the peak for 8 ML do not appear in our spectrum. Instead, sixty percent of the total integrated intensity is emitted in peaks labelled QW1 and QW2 in this sample. The peak energies for bands QW1 and QW2 are in between those measured for 5 and 10 Å thick InAs/InP QWs represented in Figure 2(b).<sup>22</sup> As expected, they are also narrower, with full widths at half maximum around  $\text{FWHM} \sim 15$  and 12 meV, respectively, than the inhomogeneously broadened QWR emission bands ( $\text{FWHM} > 22$  meV). As explained above, we tentatively assign these two peaks to radiative recombination in monolayer fluctuations of a residual InAs wetting layer.

In Figure 3, the high resolution PL spectrum obtained with our confocal setup at 5 K is compared with the ensemble averaged spectrum. The initial broad bands (dashed lines) are resolved into different sharp resonances at each specific location in the sample surface. This occurs both for the low energy components, QWR1-3, as for the higher energy bands, QW1 and QW2. For the latter, it reveals that local fluctuations of the wetting layer thickness give rise to interface islands of varying lateral extent. However, our more relevant findings are in the low energy part of the spectrum. Without additional

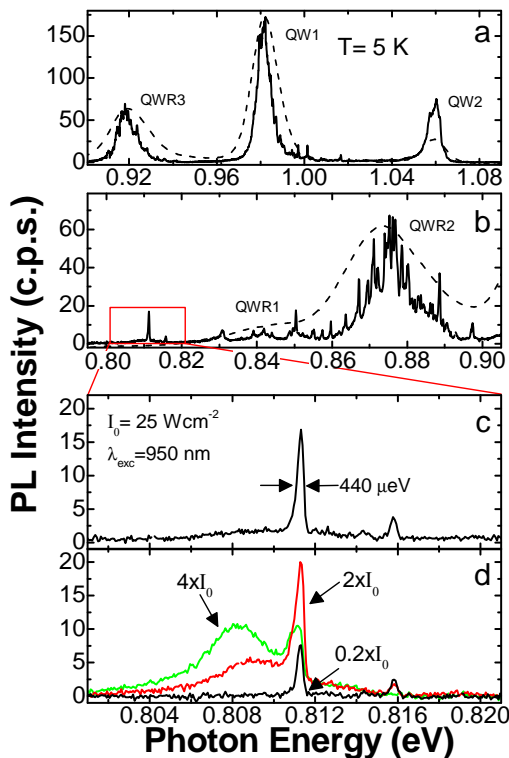


FIG. 3: a) and b) High resolution PL spectra measured at 5 K (solid lines) are compared with the inhomogeneously broadened emission bands (dashed lines). On the low energy tail, the emission from single QWRs can be studied individually as shown in b) and c). d) Evolution of the single QWR PL spectrum obtained increasing the excitation power density.

sample processing, in this region, the size inhomogeneity and the low areal density can be exploited to study the emission of specially large single QWRs [Figure 3(b), rectangle].

Laser excitation below the InP bandgap produces intense and sharp emission lines near  $1.55 \mu\text{m}$ . For the spectrum shown in Figure 3(c), the resonance linewidth is  $\sim 440 \mu\text{eV}$ , which is around twice our spectral resolution. Indeed, the main emission peak is strongly asymmetric towards lower energies. Assuming a radiative limited linewidth alone, which in any case should produce a lorentzian lineshape, it would imply an unreasonably small value of  $\sim 1.5 \text{ ps}$  for the exciton radiative lifetime. Our result rather suggest that the homogeneous linewidth in our QWRs is not radiative limited as usually reported for QDs. Moreover, increasing the laser intensity, the emission saturation behavior depicted in Figure 3(d) does not follow the typical exciton-biexciton recombination dynamics commonly observed for InAs/InP QDs.<sup>1,2,3,4,5</sup> The large aspect ratio of these QWRs suggest that they could be on a different confinement regime. Our present results indicate that this is the case concerning their non-linear emission properties. Two regimes

can be identified depending on the saturation behavior of the main peak. Initially, the integrated intensity of the sharp resonance increases almost linearly with an exponent  $m=0.98$ . At the lowest powers, the minimum achieved linewidth is limited by our spectral resolution. However, raising the excitation density slightly, the resonance asymmetry becomes patent even before the peak intensity has got completely saturated. The spectrum in Figure 3(c) is representative of this regime. Further power increase comes along with the appearance of a noticeable broad sideband shifted in energy from the main peak. In this regime, the sideband integrated intensity raises sublinear with  $m=0.8$  and shifts to lower energies while the main peak gets quenched at its original energy position. Finally, at higher power (not shown), or under non-resonant excitation, each sharp feature disappears embedded by its associated broad sideband (FWHM $\sim 4 \text{ meV}$ ).

In semiconductor QWRs, the many body correlations present among excitons and free electron-hole pairs (EHP) lead to strongly modified optical absorption and gain spectra when increasing the EHP density.<sup>23,24,25</sup> The electron and hole Coulomb interaction is screened by the photogenerated plasma causing the reduction of the exciton oscillator strength. This reduction partially cancels the band gap renormalization effect leaving the exciton energy unchanged when increasing power. Our results shown in Figure 3(d) evidence a clear reduction of the exciton resonance intensity at constant energy in favor of an increasingly broad emission band appearing at nearby energies. These spectral features must be explained assuming for our nanostructures a quasi-1D confining potential consistent with their elongated shape. They are comparable to similar optical features reported for other semiconductor QWRs based in the GaAs/AlGaAs heteroepitaxial system.<sup>16,18</sup> Compared with them, the QWRs presented here can be fabricated by a self-assembled process in nominally flat InP(001) substrates, avoiding any prepatterning and/or regrowth steps, and making easier their implementation in current photonic and optoelectronic telecommunication devices.

To conclude, we have demonstrated that isolated InAs self-assembled quantum wires can be grown in nominally flat InP(001) substrates using conventional epitaxial techniques. Emission spectra from individual QWRs have been reported in the wavelength region of interest for optical communications. Preliminary investigation of their optical properties reveals spectral signatures of the many-body carrier interactions occurring in 1D systems.

The authors gratefully acknowledge financial support by the Spanish MEC and CAM through projects NANOSELF2, NANIC and QUOIT (TEC-2005-05781-C03-01/03, NAN2004-09109-C04-01/03 and S-505/ESP/000200), and by the European Commission through SANDIE Network of Excellence (No. NMP4-CT-2004-500101).

- 
- \* benito@imm.cnm.csic.es
- <sup>1</sup> T. Mensing, L. Worschech, R. Schwertberger, J. P. Reithmaier, and A. Forchel, *Appl. Phys. Lett.* **82**, 2799 (2003).
  - <sup>2</sup> D. Chithrani, R. L. Williams, J. Lefebvre, P. J. Poole, and G. C. Aers, *Appl. Phys. Lett.* **84**, 978 (2004).
  - <sup>3</sup> K. Takemoto, Y. Sakuma, S. Hirose, T. Usuki, and N. Yokoyama, *Jpn. J. Appl. Phys.* **43**, L349 (2004).
  - <sup>4</sup> B. Salem, N. Chauvin, T. Benyattou, G. Guillot, C. Bru-Chevalier, G. Bremond, C. Monat, P. Rojo-Romeo, and M. Gendry, *Nanotechnology* **16**, 444 (2005).
  - <sup>5</sup> G. Saint-Girons, N. Chauvin, A. Michon, G. Patriarche, G. Beaudoin, G. Brémond, C. Bru-Chevallier, and I. Sagnes, *Appl. Phys. Lett.* **88**, 133101 (2006).
  - <sup>6</sup> H. Li, J. Wu, Z. Wang, and T. Daniels-Race, *Appl. Phys. Lett.* **75**, 1173 (1999).
  - <sup>7</sup> C. Walther, W. Hoerstel, H. Niehus, J. Erxmeyer, and W. T. Masselink, *J. Cryst. Growth* **209**, 572 (2000).
  - <sup>8</sup> L. González, J. M. García, R. García, J. Martínez-Pastor, C. Ballesteros, and F. Briones, *Appl. Phys. Lett.* **76**, 1104 (2000).
  - <sup>9</sup> H. R. Gutiérrez, M. A. Cotta, and M. M. G. de Carvalho, *Appl. Phys. Lett.* **79**, 3854 (2001).
  - <sup>10</sup> R. Schwertberger, D. Gold, J. P. Reithmaier, and A. Forchel, *J. Cryst. Growth* **251**, 248 (2003).
  - <sup>11</sup> D. Fuster, M. U. González, L. González, Y. González, T. Ben, A. Ponce, S. I. Molina, and J. Martínez-Pastor, *Appl. Phys. Lett.* **85**, 1424 (2004).
  - <sup>12</sup> D. Fuster, L. González, Y. González, M. U. González, and J. Martínez-Pastor, *J. Appl. Phys.* **98**, 033502 (2005).
  - <sup>13</sup> B. Alén, J. Martínez-Pastor, A. García-Cristóbal, L. González, and J. M. García, *Appl. Phys. Lett.* **78**, 4025 (2001).
  - <sup>14</sup> D. Fuster, J. Martínez-Pastor, L. González, and Y. González, *Phys. Rev. B* **71**, 205329 (2005).
  - <sup>15</sup> T. D. Harris, D. Gershoni, R. D. Grober, L. Pfeiffer, K. West, and N. Chand, *Appl. Phys. Lett.* **68**, 988 (1996).
  - <sup>16</sup> H. Akiyama, L. N. Pfeiffer, M. Yoshita, A. Pinczuk, P. B. Littlewood, K. W. West, M. J. Matthews, and J. Wynn, *Phys. Rev. B* **67**, 041302(R) (2003).
  - <sup>17</sup> A. Crottini, J. L. Staehli, B. Deveaud, X. L. Wang, and M. Ogura, *Phys. Rev. B* **63**, 121313R (2001).
  - <sup>18</sup> T. Guillet, R. Grousson, V. Voliotis, M. Menant, X. L. Wang, and M. Ogura, *Phys. Rev. B* **67**, 235324 (2003).
  - <sup>19</sup> Q. Zhu, E. Pelucchi, S. Dalessi, K. Leifer, M. A. Dupertuis, and E. Kapon, *Nano Letters* **6**, 1036 (2006).
  - <sup>20</sup> J. M. García, L. González, M. U. González, J. P. Silveira, Y. González, and F. Briones, *J. Cryst. Growth* **227-228**, 975 (2001).
  - <sup>21</sup> M. U. González, L. González, J. M. García, Y. González, J. P. Silveira, and F. Briones, *Microelectron. J.* **35**, 13 (2004).
  - <sup>22</sup> M. Hopkinson, J. P. R. David, P. A. Claxton, and P. Kightley, *Appl. Phys. Lett.* **60**, 841 (1991).
  - <sup>23</sup> S. D. Sarma and D. W. Wang, *Phys. Rev. Lett.* **84**, 2010 (2000).
  - <sup>24</sup> D. W. Wang and S. D. Sarma, *Phys. Rev. B* **64**, 195313 (2001).
  - <sup>25</sup> P. Huai and T. Ogawa, *J. of Luminescence* **119-120**, 468 (2006).